Supporting Information

Molecular Property Prediction for Very Large Databases with Natural Language Processing: A Case Study in Ionic Liquid Design

Mood Mohan[1,*], Michelle K. Kidder[2], Jeremy C. Smith[1,3,*]

[1] Biosciences Division and Center for Molecular Biophysics, Oak Ridge National Laboratory, Oak Ridge, Tennessee 37831, United States

[2] Department of Biochemistry and Cellular and Molecular Biology, University of Tennessee, Knoxville, Tennessee 37996, United States

[3] Manufacturing Science Division, Oak Ridge National Laboratory, Oak Ridge, Tennessee 37831-6201, United States

Corresponding Author(s)

[*] E-mail: moodm@ornl.gov (M. Mohan)
smithjc@ornl.gov (J.C. Smith)

S1. Ionic Liquids Dataset

For IL surface tension, the dataset compiled consists of 2,663 data points taken from our previous work,[1,2] which was originally collected from the literature and the online ionic liquids database ILThermo v2.0.[3,4] The data set contains 370 different ILs with surface tensions measured at temperatures ranging from 263 to 533 K at constant pressure. The dataset comprises 121 unique cations, including imidazolium, ammonium, phosphonium, pyridinium, pyrrolidinium, protic, morpholinium, triazolium, piperidinium, sulfonium, quinolinium, and others, and 66 unique anions, such as carboxylates, amino acids, sulfates, phosphates, cyanates, fluorides, halides, and azolates.

The IL viscosity dataset, also taken from our previous study[5], consists of 11,721 data points covering 967 distinct ILs. The reported viscosities are at temperatures ranging from 253 K to 573 K and pressures from 60 kPa to 950000 kPa. The dataset includes 419 unique cations and 172 unique anions.

The dataset for ionic conductivity of ILs was obtained from Song et al. (2024)[6], which was compiled from NIST ILThermo v2.0 database.[3,4] This dataset comprises 5,700 data points with 414 distinct ILs (180 unique cations and 85 unique anions), covering a wide range temperatures from 208.15–528.55 K and a pressure range of 95–110 kPa. The dataset categorizes ILs into nine classes based on cation types, with imidazolium-based ILs being the most prevalent, constituting approximately 56% of the data.

The IL density dataset was compiled from NIST ILThermo v2.0[3,4] and contains a total of 52,278 data points covering 1,687 ILs (906 cations and 341 anions) at a wide range temperatures from 90 K to 573 K and a pressure range of 81.5–300000 kPa. The IL density values vary from 780 kg/m^3 to 2150 kg/m^3, which reflects extensive experimental effort in designing “task-specific ILs” for different research applications.

However, it is important to mention that certain ILs in the ionic conductivity dataset, which was obtained from Song et al. (2024)[6], contain errors in the SMILES representations. For instance, the SMILES for N-octylethylenediammonium trifluoromethanesulfonate, N-hexylethylenediammonium trifluoromethanesulfonate, and N-octylethylenediammonium trifluoroacetate are misreported as NCCNCCCCCCCC.O=S([O-])(C(F)(F)F)=O,

CCCCCCNCCN.O=S([O-])(C(F)(F)F)=O, and NCCNCCCCCCCC.[O-]C(C(F)(F)F)=O, respectively, omitting the cation component. Similarly, the melting temperature dataset from Feng et al. (2024)[7] also contains SMILES errors. For example, the SMILES for imidazolium triflate, 1-butyl-3-methylimidazolium hexafluorophosphate, and 1,8-Diazabicyclo(5.4.0)undec-7-ene 2-nitroimidazol-1-ide are inaccurately reported as c1c[nH+]c[nH]1.O=S(=O)(O)C(F)(F)F, CCCC[n+]1ccn(C)c1.F[PH](F)(F)(F)(F)F, and C1CCC2=NCCC[NH+]2CC1.O=[N+](O)c1ncc[n-]1, respectively, with missing anions and a misplacement of the cation position for 1,8-Diazabicyclo[5.4.0]undec-7-ene. These charge imbalances can compromise the accuracy of ML models, potentially leading to incorrect patterns and predict properties inaccurately on new ILs. To mitigate this issue, we have identified and corrected the charge imbalances in the SMILES representations used for our ML models.

Table S1: Number of input features in the different featurization techniques

IL Property	Featurization technique	Length of features	Experimental features (T = 1 and T + P = 2) [a]	Total features
σ, mN/m	Atom count	11	1	12
	Morgan FP	2048	1	2049
	σ-profiles	14	1	15
	Mol2vec	300	1	301
ln(η), mPa.s	Atom count	11	2	13
	Morgan FP	2048	2	2050
	σ-profiles	14	2	16
	Mol2vec	300	2	302
κ, S/m	Atom count	10	2	11
	Morgan FP	2048	2	2050
	Mol2vec	300	2	302
ρ, kg/m^3	Atom count	11	2	13
	Morgan FP	2048	2	2050
	Mol2vec	300	2	302
$\log_{10}EC_{50}$	Mol2vec	300	0	300
T_m, (K)	Mol2vec	300	0	300
	Mol2vec + atom count	311	0	311
	Mol2vec + atom count + RDKit descriptors	460	0	460
γ_{IL}^{W}	Mol2vec	300	2 + mole fraction	303

[a] T is temperature in K, and P is pressure in kPa.

Table S2. The search space and results of hyperparameter parameters for the different ML models

Property	Search space	Optimized value
Viscosity	n_estimators = *trial.suggest_int(500, 3000)* l2_leaf_reg = *trial.suggest_int(1, 11)* learning_rate = *trial.suggest_float(0.03, 0.30)* depth = *trial.suggest_int(1, 11)* random_strength = *trial.suggest_int(1, 11)* boosting_type= *trial.suggest_categorical('Ordered', 'Plain')* rsm = *trial.suggest_float(0.1, 0.9)*	n_estimators = 2798 l2_leaf_reg = 6 learning_rate = 0.1774 depth = *5* random_strength = 1 boosting_type= Plain rsm = 0.7875
Surface tension	n_estimators = *trial.suggest_int(500, 3000)* l2_leaf_reg = *trial.suggest_int(1, 11)* learning_rate = *trial.suggest_float(0.03, 0.30)* depth = *trial.suggest_int(1, 11)* random_strength = *trial.suggest_int(1, 11)* boosting_type= *trial.suggest_categorical('Ordered', 'Plain')* rsm = *trial.suggest_float(0.1, 0.9)*	n_estimators = 2998 l2_leaf_reg = 4 learning_rate = 0.1088 depth = *5* random_strength = 10 boosting_type= Plain rsm = 0.6928
Ionic conductivity	n_estimators = *trial.suggest_int(500, 3000)* l2_leaf_reg = *trial.suggest_int(1, 11)* learning_rate = *trial.suggest_float(0.03, 0.30)* depth = *trial.suggest_int(1, 11)* random_strength = *trial.suggest_int(1, 11)* boosting_type= *trial.suggest_categorical('Ordered', 'Plain')* rsm = *trial.suggest_float(0.1, 0.9)*	n_estimators = 2981 l2_leaf_reg = 6 learning_rate = 0.0731 depth = *4* random_strength = 4 boosting_type= Plain rsm = 0.3162

Density	n_estimators = *trial.suggest_int(500, 3000)* l2_leaf_reg = *trial.suggest_int(1, 11)* learning_rate = *trial.suggest_float(0.03, 0.30)* depth = *trial.suggest_int(1, 11)* random_strength = *trial.suggest_int(1, 11)* boosting_type= *trial.suggest_categorical('Ordered', 'Plain')* rsm = *trial.suggest_float(0.1, 0.9)*	n_estimators = 1362 l2_leaf_reg = 1 learning_rate = 0.1894 depth = *8* random_strength = 3 boosting_type= Plain rsm = 0.3506
Toxicity	n_estimators = *trial.suggest_int(500, 3000)* l2_leaf_reg = *trial.suggest_int(1, 11)* learning_rate = *trial.suggest_float(0.03, 0.30)* depth = *trial.suggest_int(1, 11)* random_strength = *trial.suggest_int(1, 11)* boosting_type= *trial.suggest_categorical('Ordered', 'Plain')* rsm = *trial.suggest_float(0.1, 0.9)*	n_estimators = 2113 l2_leaf_reg = 2 learning_rate = 0.2766 depth = *6* random_strength = 1 boosting_type= Ordered rsm = 0.8993
Melting temperature (regression)	n_estimators = *trial.suggest_int(500, 3000)* l2_leaf_reg = *trial.suggest_int(1, 11)* learning_rate = *trial.suggest_float(0.03, 0.30)* depth = *trial.suggest_int(1, 11)* random_strength = *trial.suggest_int(1, 11)* boosting_type= *trial.suggest_categorical('Ordered', 'Plain')* rsm = *trial.suggest_float(0.1, 0.9)*	n_estimators = 2065 l2_leaf_reg = 3 learning_rate = 0.0422 depth = *6* random_strength = 7 boosting_type= Plain rsm = 0.6165
Melting temperature (classification)	n_estimators = *trial.suggest_int(500, 3000)* l2_leaf_reg = *trial.suggest_int(1, 11)* learning_rate = *trial.suggest_float(0.03, 0.30)* depth = *trial.suggest_int(1, 11)* random_strength = *trial.suggest_int(1, 11)* boosting_type= *trial.suggest_categorical('Ordered', 'Plain')* rsm = *trial.suggest_float(0.1, 0.9)*	n_estimators = 2936 l2_leaf_reg = 4 learning_rate = 0.2609 depth = *10* random_strength = 10 boosting_type= Ordered rsm = 0.2910

	bagging_temperature = trial.suggest_float(0.0, 1.0)	bagging_temperature = 0.6599
Water activity in ILs (regression)	n_estimators = *trial.suggest_int(500, 3000)* l2_leaf_reg = *trial.suggest_int(1, 11)* learning_rate = *trial.suggest_float(0.03, 0.30)* depth = *trial.suggest_int(1, 11)* random_strength = *trial.suggest_int(1, 11)* boosting_type= *trial.suggest_categorical('Ordered', 'Plain')* rsm = *trial.suggest_float(0.1, 0.9)*	n_estimators = 1771 l2_leaf_reg = 1 learning_rate = 0.1080 depth = *10* random_strength = 7 boosting_type= Plain rsm = 0.7148
Water activity in ILs (classification)	n_estimators = *trial.suggest_int(500, 3000)* l2_leaf_reg = *trial.suggest_int(1, 11)* learning_rate = *trial.suggest_float(0.03, 0.30)* depth = *trial.suggest_int(1, 11)* random_strength = *trial.suggest_int(1, 11)* boosting_type= *trial.suggest_categorical('Ordered', 'Plain')* rsm = *trial.suggest_float(0.1, 0.9)* bagging_temperature = trial.suggest_float(0.0, 1.0)	n_estimators = 2983 l2_leaf_reg = 1 learning_rate = 0.2288 depth = *9* random_strength = 4 boosting_type= Plain rsm = 0.8095 bagging_temperature = 0.2543

Table S3: Top investigated ionic liquids for various research applications and their physiochemical properties predicted by using ML models with Mol2vec featurization technique.

IL name	ln(η), mPa.s	ρ, kg/m^3	κ, S/m	σ, mN/m	$\log_{10}EC_{50}$	T_m, K	γ_{IL}^{W}	Reference
Biomass Pretreatment								
1-ethyl-3-methylimidazolium acetate	4.77	1100.38	0.19	38.17	2.04	Liquid	Hydrophilic	[8,9]
1-ethyl-3-methylimidazolium chloride	5.32	1149.23	0.34	62.57	1.86	Solid	Hydrophilic	[10]
1-allyl-3-methylimidazolium chloride	6.71	1144.32	0.07	56.66	2.06	Solid	Hydrophilic	[11]
Choline lysinate	7.70	1123.51	0.05	41.59	1.93	Solid	Hydrophilic	[12,13]
CO_2 Capture								
1-octyl-3-methylimidazolium bis(trifluoromethylsulfonyl)amide	4.50	1340.40	0.15	31.64	1.07	Liquid	Hydrophilic	[14]
Choline glycinate	5.10	1144.84	0.06	42.63	2.21	Solid	Hydrophilic	[15]
7-methyl-1,5,7-triazabicyclo(4.4.0)dec-5-ene 2,2,2-trifluoroethan-1-olate	4.42	1316.12	0.36	42.96	2.26	Solid	Hydrophilic	[16]
1,8-diazabicyclo[5,4,0]undec-7-ene imidazole	4.75	1206.92	0.32	46.11	2.30	Solid	Hydrophilic	[17]
Electrolytes								
1-ethyl-3-methylimidazolium bis(trifluoromethanesulfonyl)imide	3.53	1453.14	0.58	36.30	1.91	Liquid	Hydrophilic	
diethyl-N-methyl-N-(2-methoxyethyl) ammonium bis(trifluoromethanesulfonyl)imide	4.26	1403.91	0.24	33.94	2.27	Liquid	Hydrophilic	[18-20]
1-butyl-3-methylpyridinium bis(trifluoromethanesulfonyl)imide	4.16	1412.61	0.25	28.16	1.56	Liquid	Hydrophilic	
1-butyl-3-methylimidazolium	4.02	1070.92	0.50	45.07	1.65	Liquid	Hydrophilic	

thiocyanate							
1-butyl-1-methylpiperidinium bis(trifluoromethanesulfonyl)imide	5.10	1380.40	0.16	34.49	2.27	Liquid	Hydrophilic
1-butyl-2,3-dimethylimidazolium bis(trifluoromethanesulfonyl)imide	4.59	1417.71	0.29	35.08	1.72	Liquid	Hydrophilic

Table S4: COSMO-RS predicted logarithmic activity coefficient and excess enthalpy of lignin in the top literature reported ILs.

Ionic liquid	ln(γ)	H^E, kcal/mol
1-ethyl-3-methylimidazolium acetate	-10.66	-6.43
1-ethyl-3-methylimidazolium chloride	-5.43	-3.37
1-allyl-3-methylimidazolium chloride	-5.03	-3.05
Choline lysinate	-8.06	-5.24

Table S5: Comparison of experimental and ML predicted IL properties, with experimental data taken from Qiu et al. (2024)[21]

IL Name	Density, kg/m^3			Melting temperatures, K	
	Exp.	ML pred.	Error, %	Exp.	ML pred
$[P_{4442}][MSA]^*$	1010.37	1013.01 ± 25.70	0.26	-73.2	Liquid
$[P_{66614}][MSA]^*$	939.11	939.15 ± 20.02	0.004	-68.9	Liquid

* The synthesizability scores of [P4442][MSA] and [P66614][MSA] range from 3 to 4, indicating that these ionic liquids are relatively easy to synthesize, as experimentally demonstrated by Qiu et al.[21]

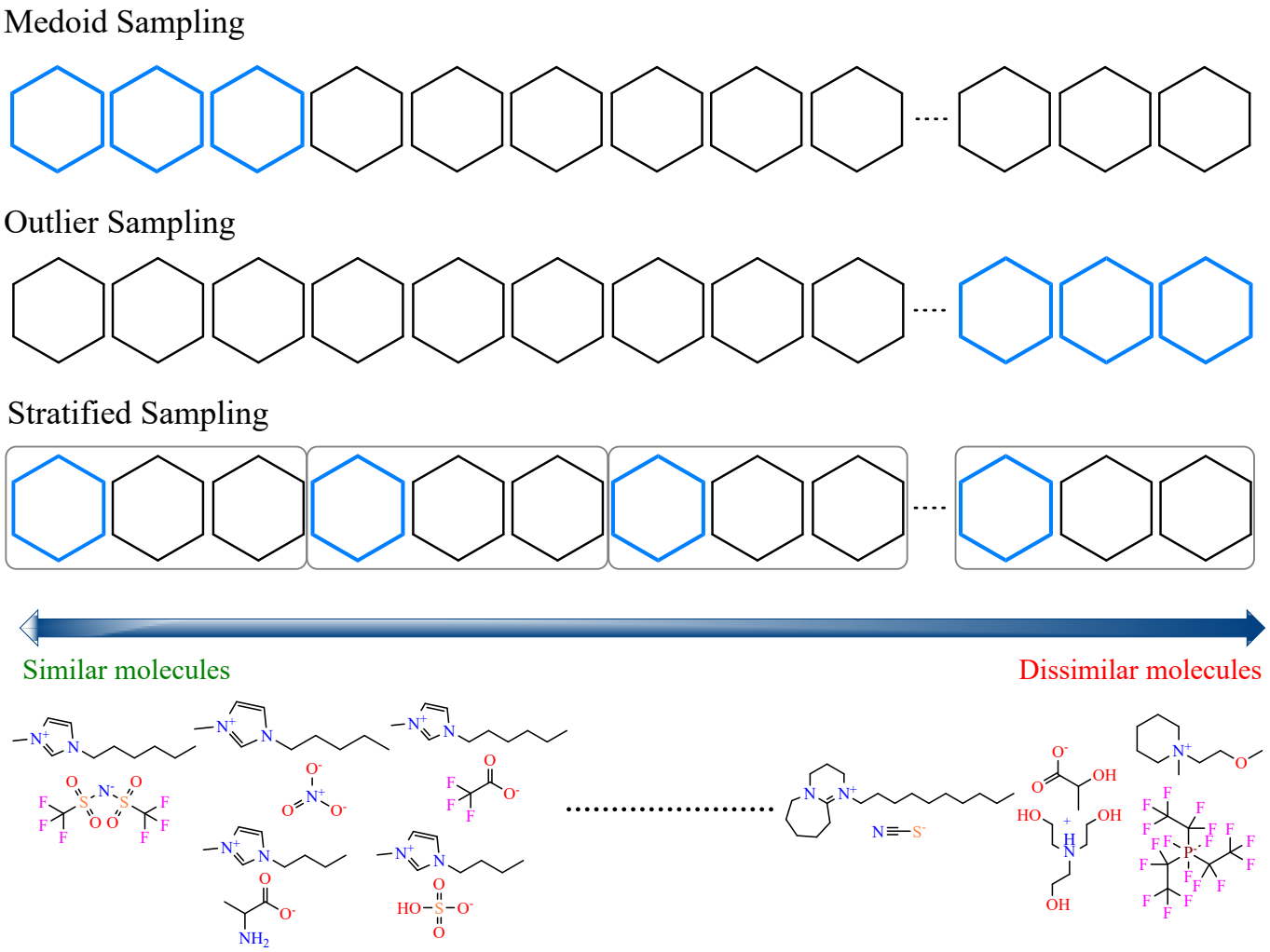

Figure S1: Graphical representation of medoid, outlier, and stratified sampling methods. The red colored arrow bar represents the chemical space of ILs, the left side of color bar corresponds to Medoid sampling (similar set of molecules), the right side of color bar corresponds to Outlier sampling (dissimilar molecules).

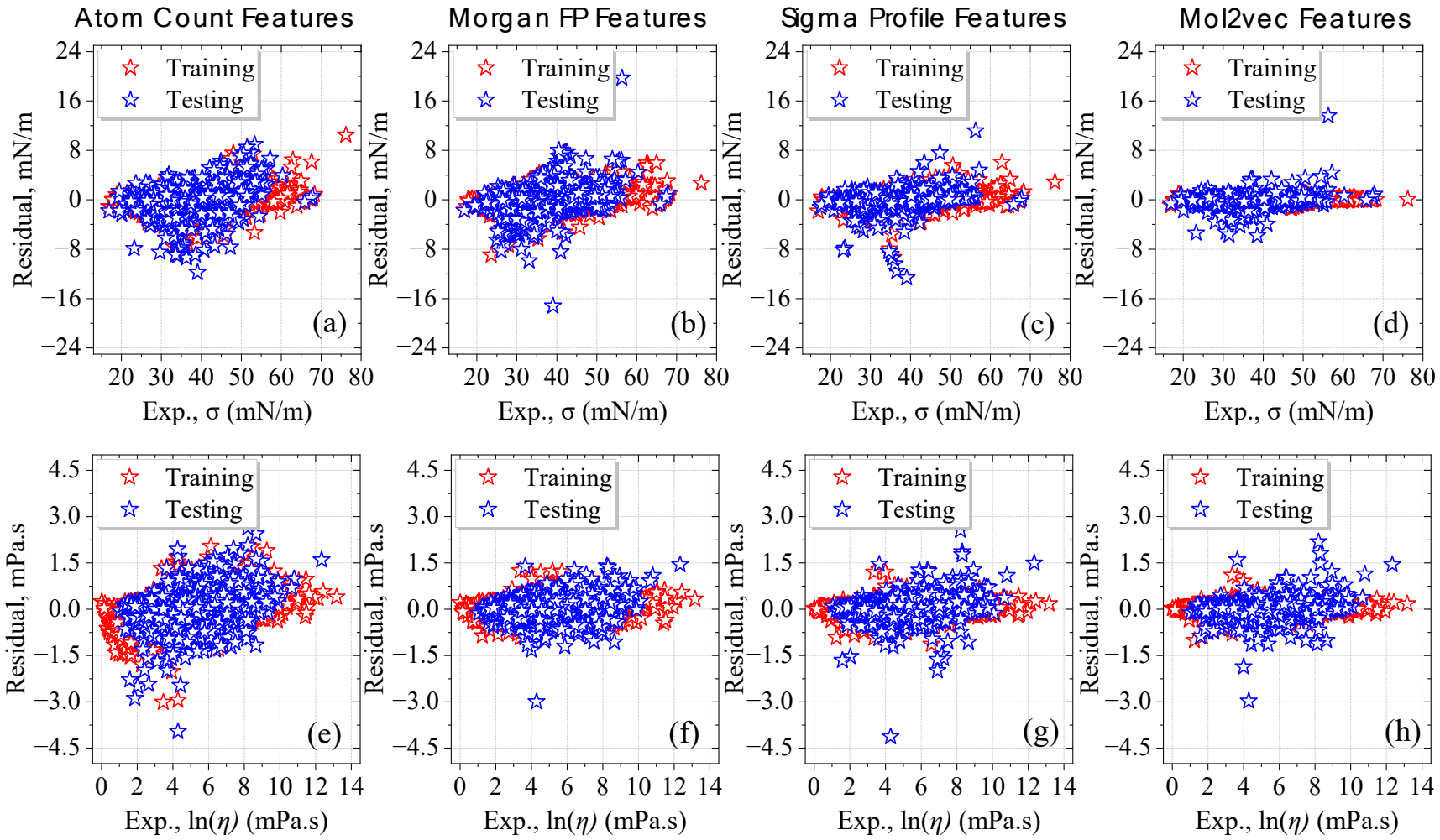

Figure S2: The relationship between residual (predicted–experimental) *vs* experimental surface tension of ILs using various approaches: (a) atom count, (b) Morgan FPs, (c) σ-profiles, and (d) Mol2vec with the CATBoost method. Similarly, the relationship between residual *vs* experimental viscosities of ILs is shown for (e) atom count, (f) Morgan FPs, (g) σ-profiles, and (h) Mol2vec featurization with the CATBoost method.

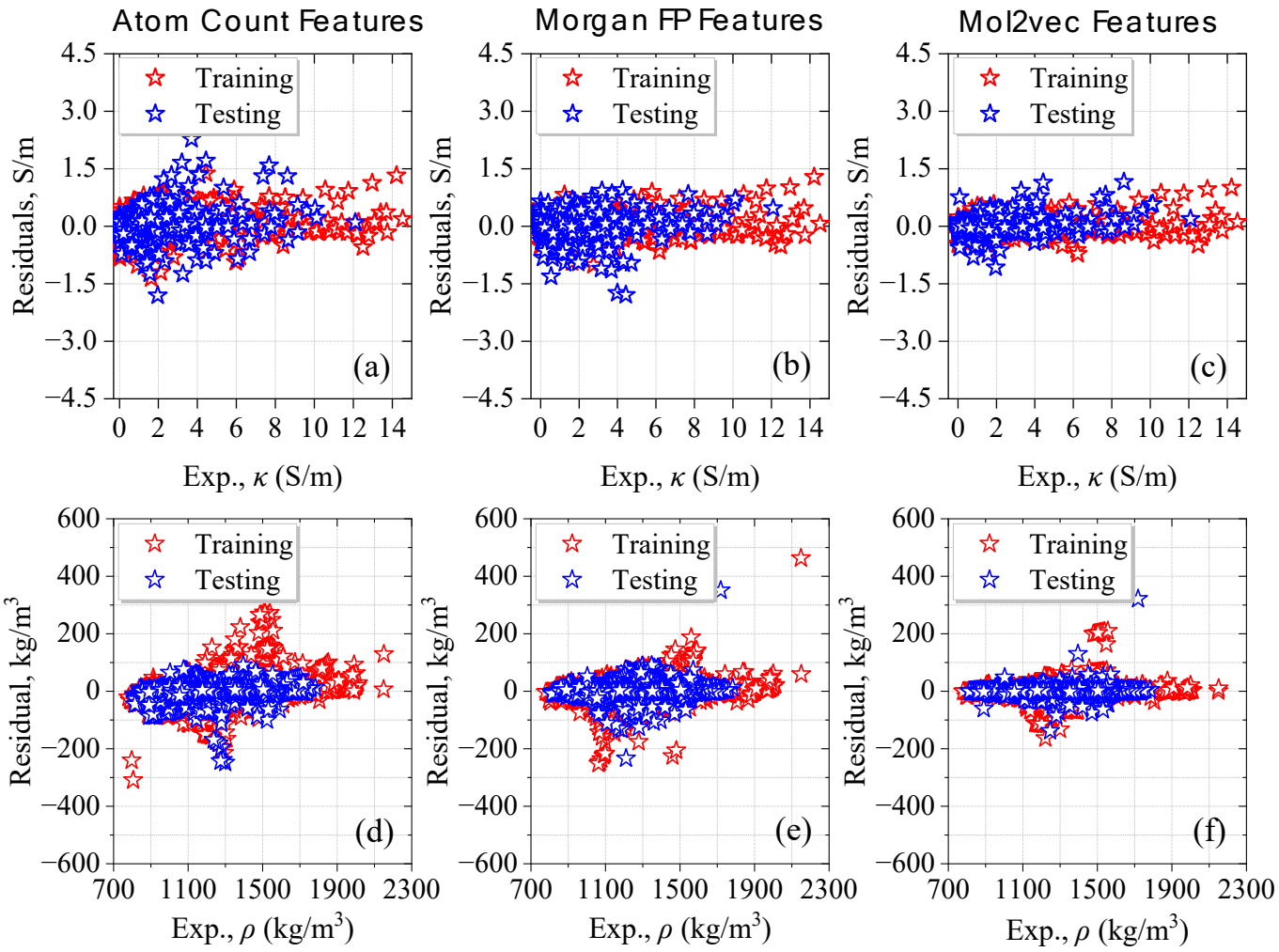

Figure S3: The relationship between residual (predicted–experimental) *vs* experimental ionic conductivity of ILs using various approaches: (a) atom count, (b) Morgan FPs, and (c) Mol2vec with the CATBoost method. Similarly, the relationship between residual *vs* experimental density of ILs is shown for (d) atom count, (e) Morgan FPs, and (f) Mol2vec featurization with the CATBoost method.

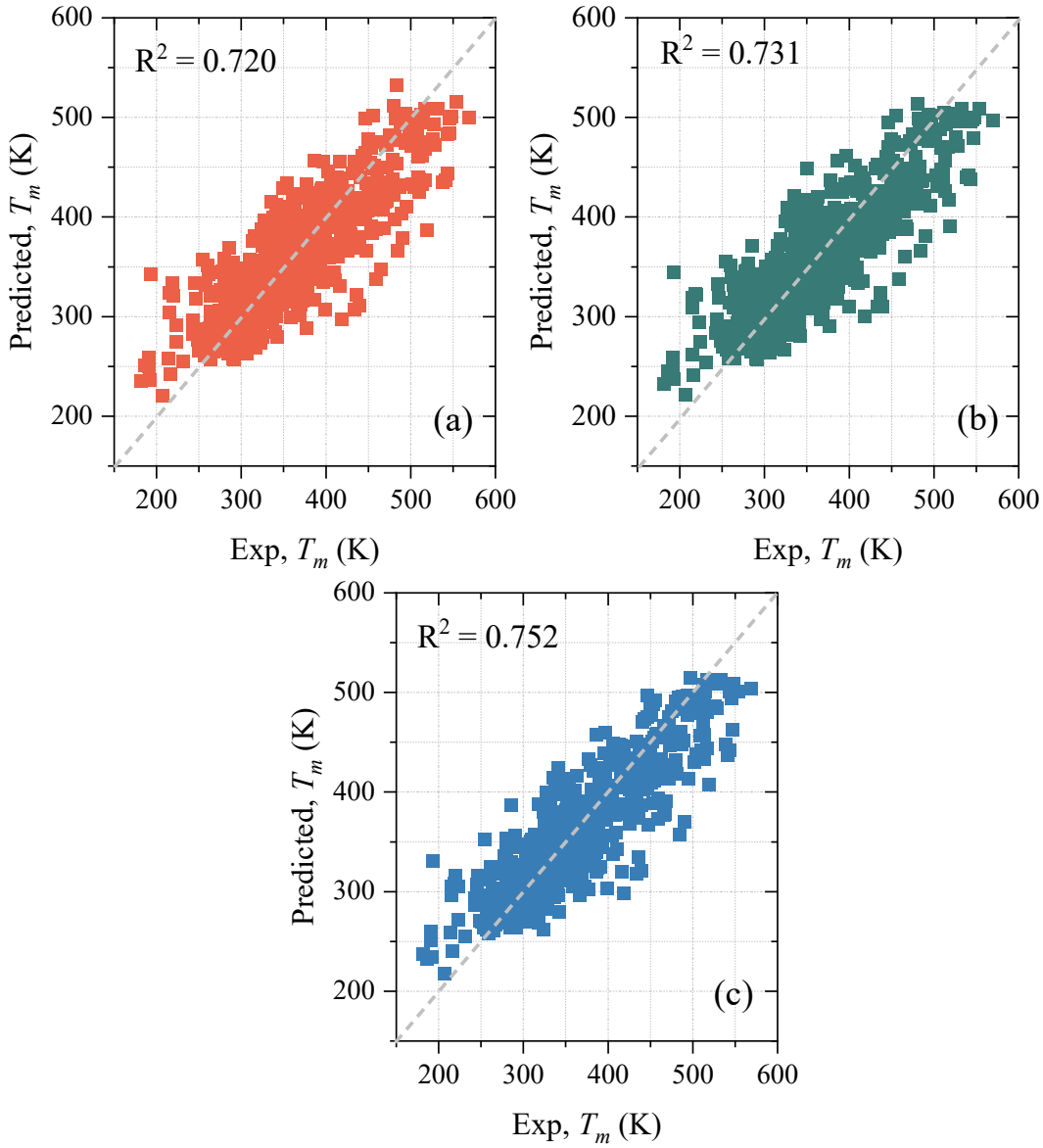

Figure S4. Experimental and ML-predicted melting temperatures of ILs using various featurizations: (a) Mol2vec features, (b) Mol2vec + atom count features, and (c) Mol2vec + atom count + RDKit molecular descriptors with the CATBoost method.

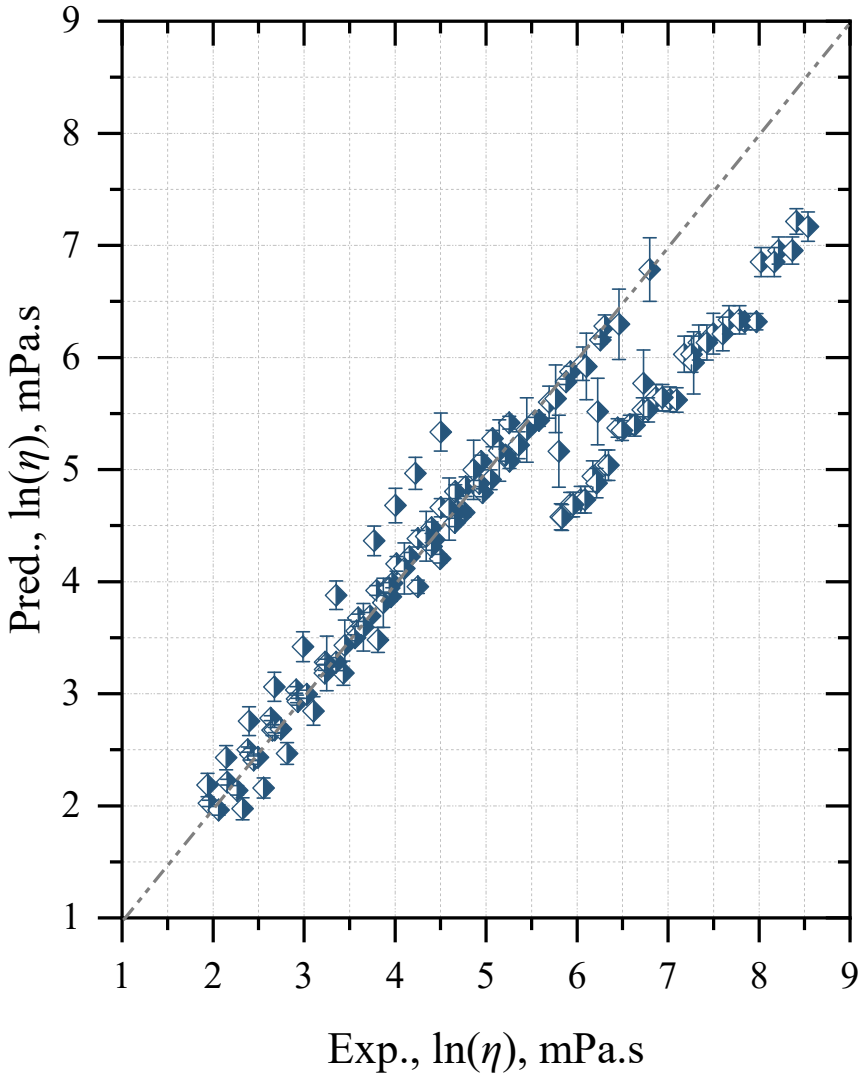

Figure S5: Performance of CATBoost model with Mol2vec features on the prediction of unseen ILs viscosity. The error bars are calculated based on the virtual ensemble (VE) module implemented in CATBoost.

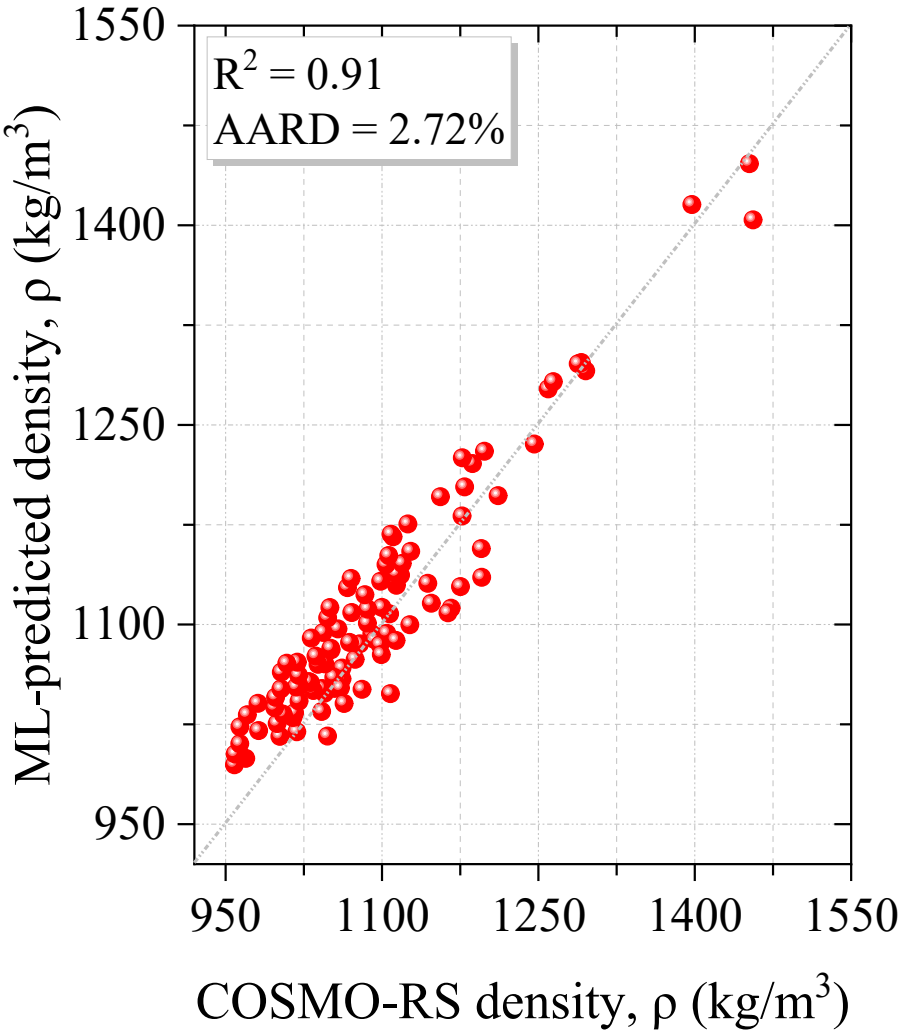

Figure S6. Correlation between the COSMO-RS calculated and newly ML predicted IL densities at 298.15 K and 101.325 kPa. The details of COSMO-RS calculations can be found in our earlier studies.[5]

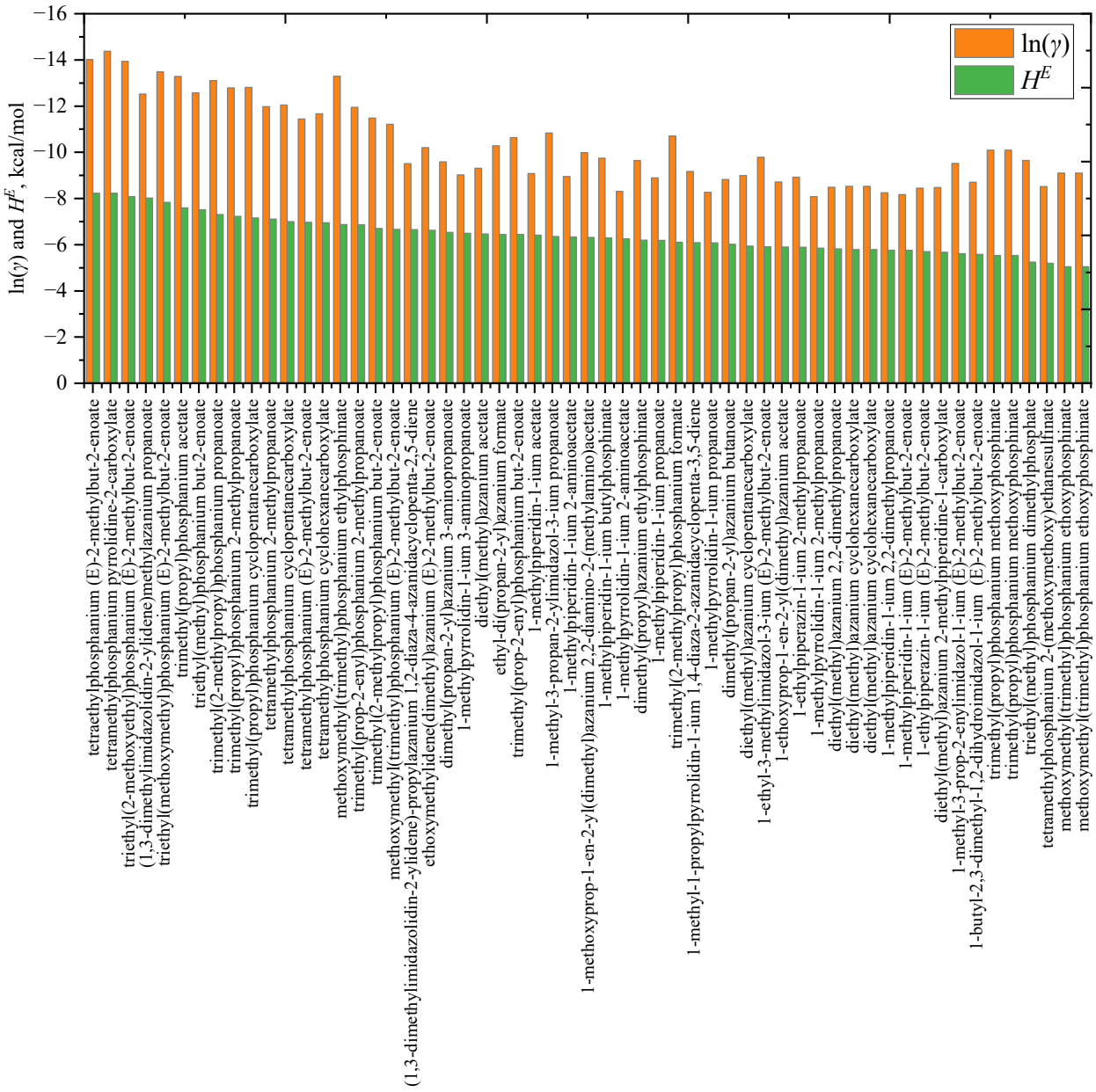

Figure S7: COSMO-RS predicted logarithmic activity coefficient (ln(γ)) and excess enthalpy (H^E) of lignin in ML developed ionic liquids with desired properties.

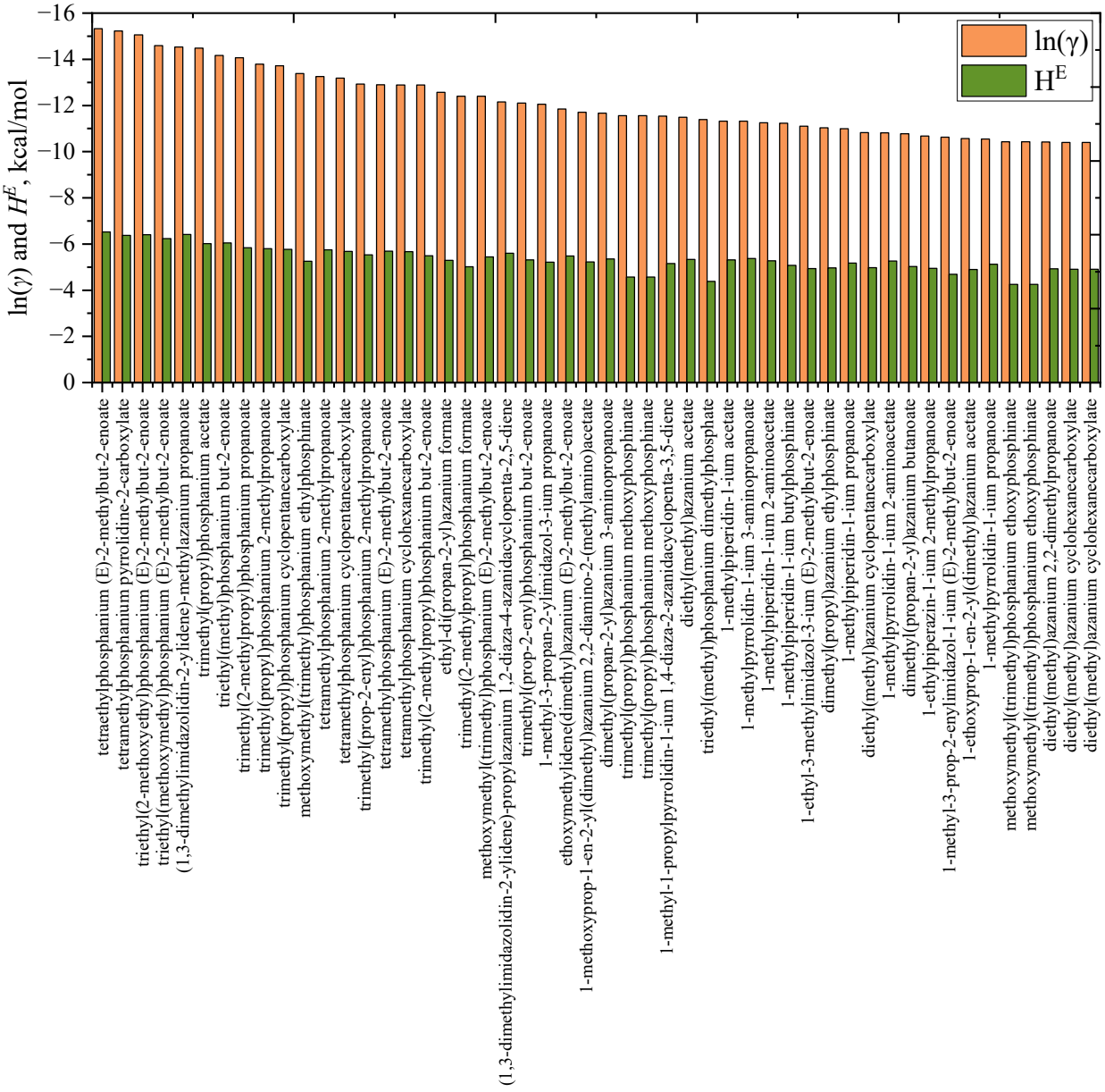

Figure S8: COSMO-RS predicted logarithmic activity coefficient (ln(γ)) and excess enthalpy (H^E) of cellulose in ML developed ionic liquids with desired properties.

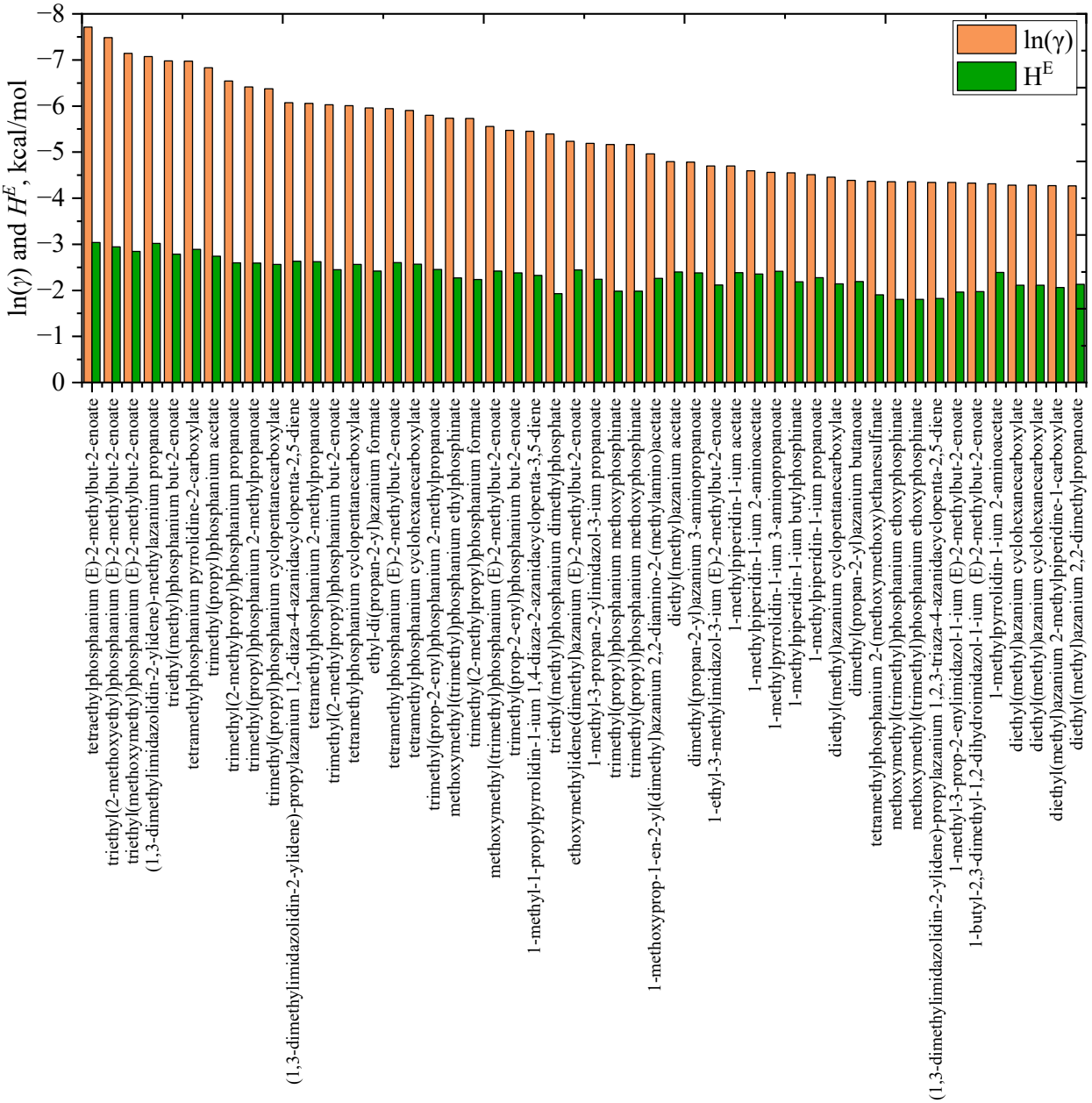

Figure S9: COSMO-RS predicted logarithmic activity coefficient (ln(γ)) and excess enthalpy (H^E) of hemicellulose in ML developed ionic liquids with desired properties.

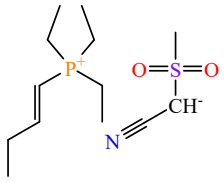

(*E*)-but-1-en-1-yltriethylphosphonium (methylsulfonyl)acetonitrile
ln(*η*) = 4.18 mPa.s; κ = 0.29 S/m

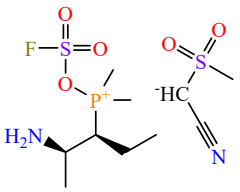

((2*R*,3*S*)-2-aminopentan-3-yl)((fluorosulfonyl)oxy)dimethylphosphonium (methylsulfonyl)acetonitrile
ln(*η*) = 3.98 mPa.s; κ = 0.20 S/m

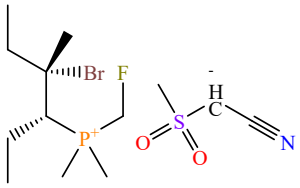

((3*R*,4*S*)-4-bromo-4-methylhexan-3-yl)(fluoromethyl)dimethylphosphonium (methylsulfonyl)acetonitrile
ln(*η*) = 4.48 mPa.s; κ = 0.23 S/m

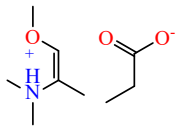

(*Z*)-1-methoxy-*N*,*N*-dimethylprop-1-en-2-aminium propionate
ln(*η*) = 3.25 mPa.s; κ = 0.32 S/m

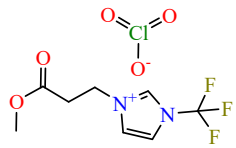

3-(3-methoxy-3-oxopropyl)-1-(trifluoromethyl)-1*H*-imidazol-3-ium chlorate
ln(*η*) = 4.42 mPa.s; κ = 0.39 S/m

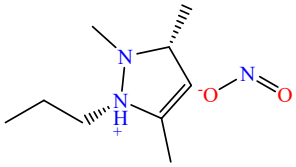

(1*S*,3*R*)-2,3,5-trimethyl-1-propyl-2,3-dihydro-1*H*-pyrazol-1-ium nitrite
ln(*η*) = 3.10 mPa.s; κ = 0.435 S/m

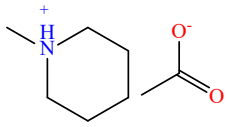

1-methylpiperidin-1-ium acetate
ln(*η*) = 2.41 mPa.s; κ = 0.30 S/m

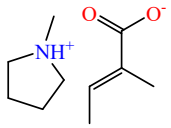

1-methylpyrrolidin-1-ium (*E*)-2-methylbut-2-enoate
ln(*η*) = 3.20 mPa.s; κ = 0.44 S/m

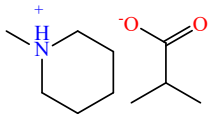

1-methylpiperidin-1-ium isobutyrate
ln(*η*) = 3.30 mPa.s; κ = 0.15 S/m

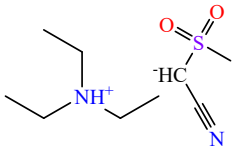

triethylammonium (methylsulfonyl)acetonitrile
ln(*η*) = 3.82 mPa.s; κ = 0.41 S/m

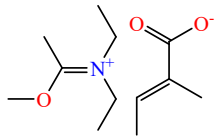

ln(*η*) = 3.85 mPa.s; κ = 0.16 S/m

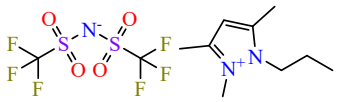

2,3,5-trimethyl-1-propyl-1*H*-pyrazol-2-ium bis((trifluoromethyl)sulfonyl)amide
ln(*η*) = 2.04 mPa.s; κ = 0.23 S/m

Figure S10: viscosity and ionic conductivity of newly engineered ionic liquids for CO_2 capture. All these ILs are predicted to be easy to synthesize with a SA score below 6.5.

References

(1) Mohan, M.; Smith, M. D.; Demerdash, O.; Kidder, M. K.; Smith, J. C. Predictive understanding of the surface tension and velocity of sound in ionic liquids using machine learning. *J. Chem. Phys.* **2023**, *158* (21), 214502. DOI: 10.1063/5.0147052.

(2) Mohan, M.; Smith, M. D.; Demerdash, O. N.; Simmons, B. A.; Singh, S.; Kidder, M. K.; Smith, J. C. Quantum chemistry-driven machine learning approach for the prediction of the surface tension and speed of sound in ionic liquids. *ACS Sustain. Chem. Eng.* **2023**, *11* (20), 7809-7821. DOI: 10.1021/acssuschemeng.3c00624.

(3) Dong, Q.; Muzny, C. D.; Kazakov, A.; Diky, V.; Magee, J. W.; Widegren, J. A.; Chirico, R. D.; Marsh, K. N.; Frenkel, M. ILThermo: A free-access web database for thermodynamic properties of ionic liquids. *J. Chem. Eng. Data* **2007**, *52* (4), 1151-1159.

(4) Kazakov, A. F.; Magee, J. W.; Chirico, R. D.; Paulechka, V.; Diky, V.; Muzny, C. D.; Kroenlein, K. G.; Frenkel, M. D. *NIST Standard Reference Database 147: NIST Ionic Liquids Database - (ILThermo). Ionic Liquids Database-ILThermo (v2. 0)*. 2021. https://ilthermo.boulder.nist.gov/ (accessed 2023 October 5).

(5) Mohan, M.; Jetti, K. D.; Guggilam, S.; Smith, M. D.; Kidder, M. K.; Smith, J. C. High-Throughput Screening and Accurate Prediction of Ionic Liquid Viscosities Using Interpretable Machine Learning. *ACS Sustain. Chem. Eng.* **2024**, *12* (18), 7040-7054. DOI: 10.1021/acssuschemeng.4c00631.

(6) Song, C.; Wang, C.; Fang, F.; Zhou, G.; Dai, Z.; Yang, Z. Large-Scale Screening for High Conductivity Ionic Liquids via Machine Learning Algorithm Utilizing Graph Neural Network-Based Features. *J. Chem. Eng. Data* **2024**.

(7) Feng, H.; Qin, L.; Zhang, B.; Zhou, J. Prediction and Interpretability of Melting Points of Ionic Liquids Using Graph Neural Networks. *ACS omega* **2024**, *9* (14), 16016-16025.

(8) Mohan, M.; Huang, K.; Pidatala, V. R.; Simmons, B. A.; Singh, S.; Sale, K. L.; Gladden, J. M. Prediction of solubility parameters of lignin and ionic liquids using multi-resolution simulation approaches. *Green Chem.* **2022**. DOI: 10.1039/d1gc03798f.

(9) Mohan, M.; Banerjee, T.; Goud, V. V. Effect of Protic and Aprotic Solvents on the Mechanism of Cellulose Dissolution in Ionic Liquids: A Combined Molecular Dynamics and Experimental Insight. *ChemistrySelect* **2016**, *1* (15), 4823-4832. DOI: 10.1002/slct.201601094.

(10) Coronado-Aldana, E. K.; Ferreira-Salazar, C. L.; Piñeros-Castro, N. Y.; Vázquez-Medina, R.; Perdomo, F. A. Thermodynamic analysis, synthesis, characterization, and evaluation of 1-ethyl-3-methylimidazolium chloride: Study of its effect on pretreated rice husk. *Chinese Journal of Chemical Engineering* **2023**, *60*, 143-154.

(11) Liu, J.-F.; Cao, Y.; Yang, M.-H.; Wang, X.-J.; Li, H.-Q.; Xing, J.-M. Enhanced saccharification of lignocellulosic biomass with 1-allyl-3-methylimidazolium chloride (AmimCl) pretreatment. *Chin. Chem. Lett.* **2014**, *25* (11), 1485-1488.

(12) Mohan, M.; Simmons, B. A.; Sale, K. L.; Singh, S. Multiscale molecular simulations for the solvation of lignin in ionic liquids. *Sci. Rep.* **2023**, *13* (1), 271. DOI: 10.1038/s41598-022-25372-2.

(13) Mohan, M.; Choudhary, H.; George, A.; Simmons, B. A.; Sale, K.; Gladden, J. M. Towards understanding of delignification of grassy and woody biomass in cholinium-based ionic liquids. *Green Chem.* **2021**, *23* (16), 6020-6035 DOI: 10.1039/d1gc01622a.

(14) Almantariotis, D.; Fandino, O.; Coxam, J.-Y.; Gomes, M. C. Direct measurement of the heat of solution and solubility of carbon dioxide in 1-hexyl-3-methylimidazolium bis [trifluoromethylsulfonyl] amide and 1-octyl-3-methylimidazolium bis [trifluoromethylsulfonyl] amide. *International Journal of Greenhouse Gas Control* **2012**, *10*, 329-340.

(15) Yuan, S.; Yang, Z.; Ji, X.; Chen, Y.; Sun, Y.; Lu, X. CO2 absorption in mixed aqueous solution of MDEA and cholinium glycinate. *Energ. Fuel* **2017**, *31* (7), 7325-7333.

(16) Dai, S.; Luo, H.; Li, H.; Wang, C.; Jiang, D. Carbon dioxide capture by superbase-derived protic ionic liquids. *Angewandte Chemie-International Edition* **2010**, *49* (34).

(17) Yan, H.; Zhao, L.; Bai, Y.; Li, F.; Dong, H.; Wang, H.; Zhang, X.; Zeng, S. Superbase ionic liquid-based deep eutectic solvents for improving CO2 absorption. *ACS Sustain. Chem. Eng.* **2020**, *8* (6), 2523-2530.
(18) Galiński, M.; Lewandowski, A.; Stępniak, I. Ionic liquids as electrolytes. *Electrochimica acta* **2006**, *51* (26), 5567-5580.
(19) Lei, Z.; Chen, B.; Koo, Y.-M.; MacFarlane, D. R. Introduction: ionic liquids. ACS Publications: 2017; Vol. 117, pp 6633-6635.
(20) Zhang, S.; Zhang, Q.; Zhang, Y.; Chen, Z.; Watanabe, M.; Deng, Y. Beyond solvents and electrolytes: Ionic liquids-based advanced functional materials. *Progress in Materials Science* **2016**, *77*, 80-124.
(21) Qiu, L.; Li, B.; Hu, J.; Ganesan, A.; Pramanik, S.; Damron, J. T.; Li, E.; Jiang, D.-e.; Mahurin, S. M.; Popovs, I. Cascade CO2 Insertion in Carbanion Ionic Liquids Driven by Structure Rearrangement. *J. Am. Chem. Soc.* **2024**, *146* (43), 29588-29598.